Intermittency in dynamical models of turbulence

Jens Eggers
Department of Mathematics, The University of Chicago, 5734 University Avenue, Chicago, Illinois 60637
and The James Franck Institute, The University of Chicago, 5640 South Ellis Avenue, Chicago, Illinois 60637
(Received 20 February 1992)

The purpose of this paper is to gain insight into the dynamical origins of intermittent fluctuations in turbulent flow. To this end stochastic models of turbulence are developed, which borrow their interaction structure from fractal geometry. The dynamics conserve energy and ensure equipartition of energy in equilibrium. The resulting stochastic process models the chaotic motion of Navier-Stokes-generated cascades [J. Eggers and S. Grossmann, Phys. Lett. **156**, 444 (1991)]. In all cases we find small-scale intermittency, but the strength of the fluctuations depends crucially on the geometry of the cascade. We calculate the variance of the energy fluctuations in a low-noise expansion and evaluate its anomalous scaling exponent to lowest order in the noise strength. The result agrees well with numerical simulations.

PACS number(s): 05.40.+j, 47.25.Cg

I. INTRODUCTION

It is believed that fluid flow $u_i(\mathbf{x},t)$ at very high Reynolds numbers is characterized in part by a series of scaling laws for the velocity structure functions

$$D^{(m)}(r)=\langle\langle\,|\mathbf{u}(\mathbf{x}+\mathbf{r},t)-\mathbf{u}(\mathbf{x},t)|^m\,\rangle\rangle \propto r^{\zeta(m)}\,. \tag{1.1}$$

Here, $\langle\langle\ \rangle\rangle$ denotes the ensemble average which at sufficiently small scales $r \ll L$ becomes translationally invariant and isotropic, independent of boundary or initial conditions. L is the length scale of energy input. Implicitly, we have also assumed that the scaling exponents $\zeta(m)$ themselves turn out to be universal.

Kolmogorov and others [1] have assumed that the energy dissipation per unit mass ε is the only relevant quantity in the scaling regime of (1.1). From this one deduces the classical scaling exponents $\zeta_{\rm cl}(m)=m/3$ and an estimate for the width of the inertial subrange, $\eta \lesssim r \lesssim L$, $\eta=(\nu^3/\varepsilon)^{1/4}$ being the Kolmogorov viscous scale. In work pioneered by Kraichnan [2–4] it was possible to derive the classical scaling law for $D^{(2)}(r)$ from a perturbative treatment of the Navier-Stokes equation. Those theories also give values for the amplitude b of the structure function $D(r)=D^{(2)}(r)=b\varepsilon^{2/3}r^{2/3}$ and refined estimates for the width of the inertial subrange [3]. However, the possibility of corrections to classical scaling was recognized early [5,6]. Subsequently, while confirming the idea of universal scaling behavior, experiments revealed small deviations from the classical scaling exponents [7,8]. Alternatively, one can look at the probability distribution of longitudinal velocity differences $\Delta u(r)=[\mathbf{u}(\mathbf{x}+\mathbf{r})-\mathbf{u}(\mathbf{x})]\cdot\mathbf{r}/r$. At large scales, $r \lesssim L$, $P(\Delta u)$ is Gaussian, while it develops increasingly stretched tails on smaller scales [8]. This means large deviations from the mean become increasingly probable at smaller scales. Those so-called intermittent fluctuations are most impressively seen in the violent bursts of the energy dissipation [9], which is sensitive to the smallest-scale movement. The entire realm of intermittency has escaped all analytical treatment of the Navier-Stokes equation, either by renormalization-group methods [10,11] or study of higher-order perturbation theory [4].

In particular, after the original description of Kolmogorov and Oboukhov was given a geometrical interpretation by Mandelbrot [12], many authors [13–17] tried to work their way backwards by starting with a phenomenological description of a turbulent field, disregarding the dynamical origins. Those models are organized in trees. The physical picture is that of a large scale eddy occupying a box of size L^3. It decays into eight smaller eddies, located in subboxes of size $(L/2)^3$. This process is repeated until the cutoff scale η is reached. Each decay process is described by a stochastic variable, which multiplies the velocity of the top eddy to give the velocity at the next step. Self-similarity is ensured by choosing the multipliers independently and with the same distribution at each step. If the distribution has a finite width, this will naturally lead to increasing fluctuations at smaller scales. There are a variety of models which describe experiments quite well [9], once the multiplier distribution is fitted to experiment. Yet, leaving experimental evidence aside,they are all consistent with no intermittency at all, and therefore cannot give any insight whatsoever into the dynamical origins of intermittency.

Reconsidering the original question of dynamics on the basis of fractal turbulence models, there are two issues.

(1) Can the geometrical (tree) structure of turbulence models be motivated on the basis of the Navier-Stokes equation?

(2) If locality of interactions is assumed, are there genuinely dynamical consequences of the hierarchical structure of the velocity field?

In a very recent paper [18] we focused on (2) by analyzing the Navier-Stokes equation in a mode decomposition of both Fourier and real space, which exactly corresponds to the structure described above. The resulting system of nonlinear ordinary differential equations shows intermittency, i.e., deviations of $\zeta(m)$ from $m/3$ and

stretched exponential tails in the probability distributions. There are no adjustable parameters, so intermittency appears here as a natural consequence of Navier-Stokes dynamics on a fractal structure.

In the following, we will disregard (1) entirely but rather study the *dynamical* mechanisms which lead to intermittency given a fractal structure. Specifically, we ask what aspects of the nonlinear dynamics are essential for the phenomenon to occur. To this end, we introduce a Langevin description of a turbulent cascade, which only incorporates three features of Navier-Stokes dynamics: (i) energy conservation, (ii) local scaling of energy transfer with energy, and (iii) return to absolute equilibrium [19]. The turbulent eddies, which in this description are represented only by their energy, will be connected into three different structures. (a) The full multifractal tree, which in Fig. 1 is shown in one dimension, thus with only two subeddies instead of eight. (b) The linear, "monofractal" chain, shown in Fig. 2. It comes out of the multifractal tree by imposing periodic boundary conditions on each level, thus forcing all amplitudes on one level to be the same. (c) The renormalized linear chain, represented in Fig. 3. It was argued in [18] that the dynamics of the full tree can be replaced by the dynamics of a linear chain with *renormalized* chain elements. This means that because the interactions are local in space, the eddies influence themselves only over finite distances in space. On the level of approximation of Fig. 3 all *spatial* interactions up to twice the eddy size are represented correctly, more distant interactions are represented by an eddy viscosity (wiggly lines in Fig. 3).

The main results and outline of the paper are as follows. In Sec. II, we present the stochastic process which gives the energy transfer between two eddies. Together with the connectivity of the eddies, this completely specifies the dynamics of the entire system. The next section contains the main body of our analytical work. We derive a Langevin description for the cascades and set up an expansion in the noise strength. Even in linear approximation there appear logarithmic corrections to the classical power laws.

In Sec. IV, simulations of the three different cascades

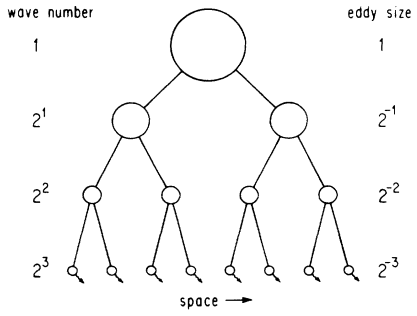

FIG. 1. The coupling structure of the *multifractal tree.* Each "eddy" (represented by a bubble) has eight subeddies, two of which are indicated here for simplicity. In the equations of motion, each bubble is represented by the value of its energy. The wavy lines on the lowest level indicate draining of energy by eddy viscosity.

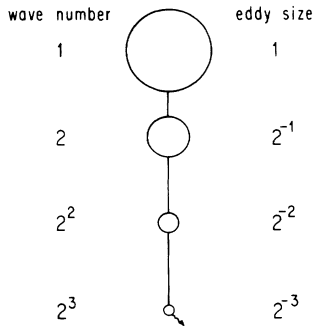

FIG. 2. The bubbles of Fig. 1 are connected into a *linear chain,* drained at the last cascade step. One can think of this structure as stemming from the tree by forcing all modes in the horizontal to be the same.

are described. We confirm our previous conjecture that the small-scale dynamics of the multifractal tree is well described by the corresponding dynamics of the renormalized chain. Hence, in the case of local coupling, it is always sufficient to study linear chains with appropriate chain elements. All those chains exhibit intermittent fluctuations well described by power-law corrections to the classical scaling laws, remnants of which appeared as logarithmic singularities in the preceding section. Yet the different chain elements differ vastly in their effectiveness to amplify fluctuations. In the case of the simple chain of Fig. 1 the effect is so small that it was previously hidden by numerical uncertainty [20]. On the other hand, for the renormalized chain intermittency effects are of similar magnitude to those found in experiment [7].

In the concluding discussion we compare the results with our earlier cascade simulations, based on the Navier-Stokes equation [18,20]. At least in the energy variables considered here our stochastic process describes the chaotic motion of a much higher-dimensional system very well. Next we discuss the significance of the energy description for the appearance of logarithmic singularities. Finally, we indicate directions of future research.

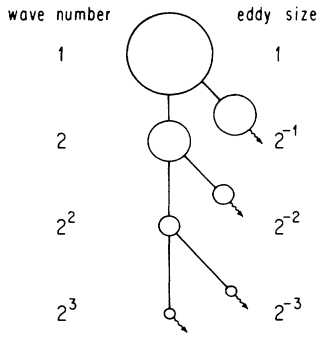

FIG. 3. The *renormalized linear chain.* It is derived from the multifractal tree by a pruning procedure which preserves the local coupling structure. At each stage, the right half of the tree is represented by an eddy viscosity with a renormalized coupling constant $D(l)$.

II. THE MODEL EQUATIONS

In the following, the only dynamical variable will be the energy of the different eddies. To simplify the subsequent considerations, let us consider a linear chain of N_η eddies with energies $E_1 \ldots, E_{N_\eta}$, which are coupled by nearest-neighbor interactions. The dynamical equations are then the energy-balance equations

$$E_l(t_{n+1}) - E_l(t_n) = \Delta E_{l-1\to l}(t_n) - \Delta E_{l\to l+1}(t_n) \ . \tag{2.1}$$

To close this set of equations, the $\Delta E_{l-1\to l}(t_n)$ will be prescribed stochastic processes, which depend only on the energies E_{l-1} and E_l of the eddies between which energy is transferred. We further demand the rate of energy transfer to be a homogeneous function of E_{l-1} and E_l. Each of the transfers between levels has its own time stepping. Since time has dimensions of (length)/(energy)$^{1/2}$, the time steps are

$$\Delta t_n^{l-1\to l} = t_{n+1}^{l-1\to l} - t_n^{l-1\to l} = 2^{-(l-1)}[E_{l-1}(t_n^{l-1\to l})]^{-1/2} \times \tau\left[\frac{E_l(t_n^{l-1\to l})}{E_{l-1}(t_n^{l-1\to l})}\right] \ . \tag{2.2}$$

The chain is updated asynchronously at times t_n,

$$\{t_n\} = \bigcup_{l=1}^{N_\eta} \{t_n^{l-1\to l}\} \ , \quad t_{n+1} > t_n \ .$$

The energy transfer at time t_n therefore is

$$\Delta E_{l-1\to l} = \begin{cases} E_{l-1}(t_n)\varphi\left[\dfrac{E_l(t_n)}{E_{l-1}(t_n)}\right]\zeta_l & \text{if } t_n = t_n^{l-1\to l} \\ 0 \quad \text{if } t_n \neq t_n^{l-1\to l} \ . \end{cases} \tag{2.3}$$

In our computations we will choose φ and τ such that $\Delta E_{l-1\to l}$ and $\Delta t_n^{l-1\to l}$ are symmetric in E_{l-1} and E_l:

$$\varphi(V) = \varphi_0 V^{1/2} \tag{2.4}$$

and

$$\tau(V) = \tau_0 V^{-1/4} \ . \tag{2.5}$$

The direction of the transfer is given by the random variable ζ_l, which takes the value $\zeta = +1$ (forward transfer) with probability p and $\zeta = -1$ (backward transfer) with probability $1-p$. If $p > \frac{1}{2}$ this will lead to an average energy transfer down to smaller scales. On the other hand, it is easy to see that constant p will lead to an unstable system: There are no restoring forces and diffusion will eventually make the energy arbitrarily large or negative. To find the right dependence of p on E_{l-1} and E_l we invoke the concept of absolute equilibrium [19]. Without viscosity and forcing one would assume all the energies to exhibit equipartition, i.e., to be the same on the average. This property can actually be confirmed for our simplified Navier-Stokes cascades [20,18]. This means the interaction is such that energies always relax towards equilibrium. This is ensured by

$$p = p\left[\frac{E_l}{E_{l-1}}\right] \ , \quad p(0) = 1 \ , \quad p(\infty) = 0 \ , \quad p(1) = \tfrac{1}{2} \ . \tag{2.6}$$

The most natural choice seems to be $(1-p)/p = V^s$ or

$$p(V) = \frac{1}{1+V^s} \ . \tag{2.7}$$

The exponent s controls how effectively the system tends to equilibrium. If s equals 0, there is no restoring "force"; for increasing s this force becomes larger.

This completes the description of the dynamics of the chain. A nonequilibrium state is maintained by feeding energy at rate ε into the chain. This is done by injecting an energy amount ε into E_1 in time steps of one. Those time steps also serve as a clock relative to which all other time steps are determined.

Usually viscous dissipation serves as an energy sink, which ensures that a stationary state is maintained. In the present model this is difficult to implement, since the energies for the dissipation region would come close to the singular point $E_l = 0$. Instead we terminate the cascade by introducing an eddy viscosity into level N_η, which simulates the action of lower-lying eddies [21,18].

The equation for $E_{N_\eta}(t_n)$ is therefore

$$E_{N_\eta}(t_{n+1}) - E_{N_\eta}(t_n) = \Delta E_{N_\eta - 1\to N_\eta}(t_n) - \Delta E_{N_\eta}^D(t_n) \ . \tag{2.8}$$

The time steps for $\Delta E_{N_\eta}^D$ are taken to be $\Delta t_n^{N_\eta - 1\to N_\eta}$, and the energy transported in one time step is

$$\Delta E_{N_\eta}^D = D E_{N_\eta} \ , \tag{2.9}$$

which is a positive-definite quantity.

The equations for a linear chain are easily generalized to the case of a multifractal tree. Let $E_l^{(i)}$, $1 \le i \le 8^{l-1}$ be the energy of the ith eddy on the lth level. Then the energy-balance equation reads

$$E_l^{(i)}(t_{n+1}) - E_l^{(i)}(t_n) = \Delta E_{l-1\to l}^{(i)}(t_n) - \sum_{i^-} \Delta E_{l\to l+1}^{(i)}(t_n) \ . \tag{2.10}$$

Here i^- are the indices of the eight eddies below i. $\Delta E_{l-1\to l}^{(i)}$ is chosen to be exactly the same as $\Delta E_{l-1\to l}$ before, with the top eddy energy $E_{l-1}^{(i^+)}$ and $E_l^{(i)}$ replacing E_{l-1} and E_l in the case of the linear chain.

The equation for the renormalized linear chain should be obvious from Fig. 3. For all but one eddy at each level the downward coupling is replaced by an eddy viscosity, as given by (2.9). The constant D is allowed to be scale dependent: $D = D(l)$.

III. LANGEVIN EQUATION AND LOW-NOISE EXPANSION

For simplicity, in this section we will consider only the linear chain, as described by (2.1). In deriving the corresponding Langevin equation, we will always assume that the individual energies E_l are much larger than the jumps: $E_l \gg \Delta E_{l-1\to l}$. The parameters ε, φ_0, τ_0, and s have to be chosen to ensure this. Ideally, let us consider a time interval Δt with $\Delta t \gg \Delta t_n^{l-1\to l}$ and assume that

E_{l-1} and E_l can be regarded as constant over the time interval Δt. Then the total energy transferred from $l-1$ to l in Δt is

$$E_{l-1}\varphi\left[\frac{E_l}{E_{l-1}}\right]\sum_{i=1}^{[\Delta t/\Delta t_n^{l-1\to l}]}\xi_l^{(i)}=\Delta_{l-1\to l}\ , \tag{3.1}$$

where $\xi_l^{(i)}$ are the realizations of ξ_l in Δt. Since $\Delta t/\Delta t_{l-1\to l}$ is large, $\Delta_{l-1\to l}/\Delta t$ is a Gaussian random variable with mean

$$2^{(l-1)}E_{l-1}^{3/2}\varphi\left[\frac{E_l}{E_{l-1}}\right]\left[\tau\left[\frac{E_l}{E_{l-1}}\right]\right]^{-1}\langle\xi_l\rangle$$

and variance

$$\frac{1}{\Delta t}2^{(l-1)}E_{l-1}^{5/2}\varphi^2\left[\frac{E_l}{E_{l-1}}\right]\left[\tau\left[\frac{E_l}{E_{l-1}}\right]\right]^{-1}\times\langle(\xi_l-\langle\xi_l\rangle)^2\rangle\ .$$

From the definition of ξ_l we have

$$\langle\xi_l\rangle=2p\left[\frac{E_l}{E_{l-1}}\right]-1$$

and

$$\langle(\xi_l-\langle\xi_l\rangle)^2\rangle=4p\left[\frac{E_l}{E_{l-1}}\right]\left[1-p\left[\frac{E_l}{E_{l-1}}\right]\right]\ .$$

For $E_l\gg\Delta E_{l-1\to l}$ we can pass to the Langevin equation which is the continuum limit of the process (2.1):

$$\partial_t E_l=h_l(E_{l-1},E_l,E_{l+1})+g_{lk}(E_{l-1},E_l,E_{l+1})\xi_k(t)\ , \tag{3.2}$$

$$\langle\xi_k(t)\xi_k(t')\rangle=2\delta(t-t')\ . \tag{3.3}$$

Here, $\{\xi_k\}$ are independent Gaussian random variables [22].

We find for $l=2,\ldots,N_\eta-1$

$$h_l=2^l\left\{\frac{1}{2}E_{l-1}^{3/2}\psi\left[\frac{E_l}{E_{l-1}}\right]-E_l^{3/2}\psi\left[\frac{E_{l+1}}{E_l}\right]\right\} \tag{3.4}$$

and

$$g_{lk}=2^{l/2}\left\{\delta_{lk}E_{l-1}^{5/4}\chi\left[\frac{E_l}{E_{l-1}}\right]-\delta_{lk-1}\sqrt{2}E_l^{5/4}\chi\left[\frac{E_{l+1}}{E_l}\right]\right\}, \tag{3.5}$$

where we have set

$$\psi(V)=\psi(V)[2p(V)-1]/\tau(V)$$

and

$$\chi(V)=\varphi(V)\{p(V)[1-p(V)]/\tau(V)\}^{1/2}\ .$$

For $l=1$ we have

$$h_1=\varepsilon-2E_1^{3/2}\psi\left[\frac{E_2}{E_1}\right], \tag{3.6}$$

$$g_{1k}=-2\delta_{2k}E_1^{5/4}\chi\left[\frac{E_2}{E_1}\right], \tag{3.7}$$

and the eddy viscosity in level N_η leads to

$$h_{N_\eta}=2^{N_\eta}\left[\frac{1}{2}E_{N_\eta-1}^{3/2}\left\{\psi\left[\frac{E_{N_\eta}}{E_{N_\eta-1}}\right]-D\frac{E_{N_\eta}}{E_{N_\eta-1}}\left[\tau\left[\frac{E_{N_\eta}}{E_{N_\eta-1}}\right]\right]^{-1}\right\}\right], \tag{3.8}$$

$$g_{N_\eta k}=2^{N_\eta/2}\left[\delta_{N_\eta k}E_{N_\eta-1}^{5/4}\left\{\chi\left[\frac{E_{N_\eta}}{E_{N_\eta-1}}\right]-D\frac{E_{N_\eta}}{E_{N_\eta-1}}\left[\tau\left[\frac{E_{N_\eta}}{E_{N_\eta-1}}\right]\right]^{-1/2}\right\}\right]. \tag{3.9}$$

We have not been able to compute the stationary energy distribution of the nonlinear system of Langevin equations (3.2) exactly. Instead, we will set up a perturbation theory in the strength of the noise [23] and calculate the results to first order.

The idea is to write the solution $E_l(t)$ as a series

$$E_l(t)=E_l^{(0)}(t)+\delta E_l^{(1)}(t)+\cdots\ , \tag{3.10}$$

where we have introduced an expansion parameter δ. Rescaling time and energy according to $\hat{t}=t/\tau_0$ and $\hat{E}_l=E_l\varphi_0^2$ we obtain

$$\partial_{\hat{t}}\hat{E}_l=\hat{h}_l(\hat{E}_{l-1},\hat{E}_l,\hat{E}_{l+1})+\delta\hat{g}_{lk}(\hat{E}_{l-1},\hat{E}_l,\hat{E}_{l+1})\hat{\xi}_k\ , \tag{3.11}$$

$$\langle\hat{\xi}_k(\hat{t})\hat{\xi}_k(\hat{t}')\rangle=2\delta(\hat{t}-\hat{t}')\ , \tag{3.12}$$

with

$$\delta=\varphi_0^{1/2}\ ,\qquad \hat{\varepsilon}=\varepsilon\tau_0\varphi_0^2\ . \tag{3.13}$$

Here $\hat{h}_l$ and $\hat{g}_{lk}$ are the previous functions h_l and g_{lk} with $\hat{\varepsilon}$ instead of ε and $\tau_0=\varphi_0=1$. For the rest of this section we will omit the carets and assume that all quantities have already been properly scaled.

The lowest order is obtained by formally setting $\delta=0$, which gives the deterministic motion

$$\partial_t E_l^{(0)}=h_l(E_{l-1}^{(0)},E_l^{(0)},E_{l+1}^{(0)}) . \tag{3.14}$$

Let us consider only the stationary behavior, $\partial_t E_l^{(0)}=0$. Seeking solutions of the form $E_l^{(0)}=C2^{-(2/3)l}$ we find

$$C=\left[\frac{\varepsilon}{\psi(2^{-2/3})}\right]^{2/3} . \tag{3.15}$$

The equation for the first order in δ is [23]

$$\partial_t E_l^{(1)}=-\gamma_{lk}E_k^{(1)}+g_{lk}(E_{l-1}^{(0)},E_l^{(0)},E_{l+1}^{(0)})\xi_k \tag{3.16}$$

with

$$\gamma_{lk}=-\frac{\partial}{\partial E_k}h_l|_{E_k=E_k^{(0)}} . \tag{3.17}$$

The covariance matrix $\sigma_{ij}=\langle E_i^{(1)}E_j^{(1)}\rangle$ for the stationary state is then given by [22]

$$\gamma_{il}\sigma_{lj}+\gamma_{jl}\sigma_{li}=2D_{ij} , \tag{3.18}$$

$$D_{ij}=g_{ik}\{E_l^{(0)}\}g_{jk}\{E_l^{(0)}\} . \tag{3.19}$$

Here, γ and D are tridiagonal matrices, D being symmetric.

For $i,j>1$, γ and D scale like

$$\gamma_{ij}=2^{(2/3)j}\bar{\gamma}(j-i) \tag{3.20}$$

and

$$D_{ij}=2^{-(2/3)j}\bar{D}(j-i) . \tag{3.21}$$

We solve (3.18) by diagonalizing the matrix γ^T:

$$(P^{-1})_{ki}\gamma_{ji}P_{jl}=\Lambda^{(k)}\delta_{kl} . \tag{3.22}$$

By inserting (3.22) into (3.18) we find

$$\sigma_{m_1m_2}=(P^{-1})_{k_1m_1}(P^{-1})_{k_2m_2}\frac{2P_{n_1k_1}P_{n_2k_2}}{\Lambda^{(k_1)}+\Lambda^{(k_2)}}D_{n_1n_2} . \tag{3.23}$$

Now σ_{ij} is easily computed by numerically finding the eigenvalues and eigenvectors of γ^T and applying (3.23). Naive power counting would predict σ_{ij} to behave like $2^{-(4/3)j}\bar{\sigma}(j-i)$, but even for i,j large *we find corrections to this behavior.* Concentrating on the diagonal elements we specifically find $\hat{\sigma}_{ll}=\sigma_{ll}/\langle E_l\rangle^2$ to be a *linear function* of the level number l. For the second moment of the energy E_l, normalized by $\langle E_l\rangle$, this means

$$\langle E_l^2\rangle/\langle E_l\rangle^2=1+\delta^2\hat{\sigma}_{ll} . \tag{3.24}$$

Since we expect anomalous scaling of the form $\langle E_l^2\rangle/\langle E_l\rangle^2=\text{const}2^{\alpha l}$, we exponentiate (3.24) to give

$$\langle E_l^2\rangle/\langle E_l\rangle^2=2^{\delta^2\hat{\sigma}_{ll}/\ln 2} . \tag{3.25}$$

To make contact with the scaling exponents $\zeta(m)$ defined in the Introduction, we observe that

$$\langle E_l^{m/2}\rangle\sim 2^{-l\zeta(m)} , \tag{3.26}$$

since the energy is quadratic in the velocities. Defining the asymptotic slope of $\hat{\sigma}_{ll}$ as σ, we find

$$\zeta(4)-2\zeta(2)=\delta^2\sigma/\ln 2 . \tag{3.27}$$

To lowest order, we therefore find corrections to classical scaling $\zeta_{\text{cl}}(m)=m/3$, which are quadratic in the noise strength δ.

IV. CASCADE SIMULATIONS

We now explore the scaling behavior of our model turbulence by numerical simulation. As before, we begin with the simple linear chain.

The constants to be fixed are the amplitude of the energy transfer φ_0, the corresponding time scale τ_0, and the exponent s which determines the approach to equilibrium. Finally, the eddy viscosity constant D has to be adjusted. The energy input rate ε is normalized to one. We choose the parameters to ensure that the energies transferred in one step are much smaller than the mean values of the energy in the corresponding level. If we fix $\langle E_1\rangle$ to be approximately 100, the ratio will always be on the order of 1%. We will use the result of Sec. III, $\langle E_l\rangle\approx C2^{-(2/3)l}$, so we choose

$$[\psi(2^{-2/3})]^{-2/3}=(100)2^{2/3} .$$

We also expect the time scales of the eddies to scale approximately like $2^{-(2/3)l}$ as in the Kolmogorov theory. Therefore we fix τ_0 such that

$$\Delta t_n^{1\to 2}\approx\tau_0 C^{-1/2}2^{-1/2}=2^{-2/3} .$$

The central parameter is the exponent s, which fixes the size of the fluctuations as measured by $\hat{\sigma}_{11}=\sigma_{11}/\langle E_1\rangle^2$. To fix it, one needs actual turbulence data or Navier-Stokes derived values. We choose s to make $\hat{\sigma}_{11}$ equal to the corresponding value in our cascade simulations, based on the Navier-Stokes equation [20]. The value for the truncation we call "small cascade" is $\hat{\sigma}_{11}=0.022$. From the linearized theory of Sec. III we find this value by choosing $s=0.85$.

By reasoning very much along the same lines, and assuming $\frac{2}{3}$ scaling we can also fix the value of D. All adjusted constants are compiled in the second row of Table I. The simulations were conducted with chains of 10 to 15 elements, thus covering a range of three to four decades in scale. Even allowing for end effects one can expect an inertial range of more than two decades. The quantities of main interest are the moments of $E_l^{1/2}$. Their scaling behavior (if scaling is found) corresponds to the exponents $\zeta(m)$ as given in (3.26). The time averages are typically taken over 10^6 time units. If we take $T=\langle E_1\rangle/\varepsilon=100$ to be the turnover time of the highest eddy, this corresponds to the enormous averaging time of 10^4T. This is easily achieved due to the small number of modes used to model turbulence. It is obviously numerically far more demanding to integrate a large set of nonlinear equations at each cascade step, as done in [20].

The scaling of the first and fourth moments of E_l is illustrated in Fig. 4. Apart from end effects, the moments are well described by a power-law fit. The exponents, as

TABLE I. The parameters specifying the dynamics of the four different cascades simulated. The definition of the parameters can be found in Sec. II. D^* is the fixed point of the renormalized coupling constant as explained in Sec. IV. The linear chain is simulated with two different values of s, giving different values for $\hat{\sigma}_{11}=\sigma_{11}/\langle E_1\rangle^2$, the normalized variance of the energy.

Parameter	φ_0	τ_0	S	D^*	D
Linear chain $\hat{\sigma}_{11}=0.022$	0.040 932 4	11.2246	0.85		0.01
Linear chain $\hat{\sigma}_{11}=0.063$	0.069	11.2246	0.5		0.01
Multifractal tree	0.042 1	11.2246	0.15		9.5×10^{-3}
Renormalized chain	0.0421	11.2246	0.15	9.49×10^{-3}	9.5×10^{-3}

given in Table II, are found to be very close to the classical values, yet there are small deviations. For $\zeta(18)$, the deviation is just 4% of $\zeta_{\rm cl}=6$. We have also listed the results of experiments [7] so one can appreciate the smallness of the effect. We now enhance fluctuations by lowering s to the value 0.5. For larger deviations from the mean values, nonlinear effects should become more important, hence enhancing intermittency. As is apparent from Table II, the exponent deviations from classical scaling have indeed increased significantly.

From earlier work [18] it is to be expected that intermittency is much stronger for the multifractal tree, or its linear analog, the renormalized chain. We first check the conjecture of Ref. [18], that the renormalized chain gives indeed a good description of the statistics of the full tree. It is difficult to observe scaling on the multifractal tree directly, since the number of modes grows as $(8^{N_\eta}-1)/7$ with the number of cascade steps N_η. So even for a moderately long cascade with six steps, the number of eddies is approximately 4×10^4. We therefore only simulate a multifractal tree of length $N_\eta=4$, but compare the moments directly with a renormalized chain with the same parameter values. We again set $\varepsilon=1$ and adjust the parameters such that $\langle E_1\rangle\approx100$. However, there is an important difference in the stationary states which will develop.

On the multifractal tree, the turbulent states are driven much farther away from equilibrium than in the linear case. This results from the increase in phase space volume towards smaller scales, which is correctly described by the multifractal tree. The energy *density* $(1/2^{-3l})E_l^{(i)}$ of a turbulent eddy still scales like $2^{-(2/3)l}$, but absolute equilibrium requires equal excitation of all *energies*. The ratio of energies $V=E_{l-1}^{(i^+)}/E_l^{(i)}$ is therefore enhanced by a factor of $8(2^{2/3})$ from the equilibrium situation $V=1$ instead of just $2^{2/3}$ in the linear case. As a result, the "force" restoring equilibrium is much stronger for the same s values. Hence s has to be adjusted to a much lower value to give fluctuations of the same size as for the linear chain.

This different value of s is the only thing reflecting the difference in dynamics between the linear chain and the multifractal tree. For $s=0.15$ $\hat{\sigma}_{11}$ still has the lower value of $\hat{\sigma}_{11}=0.013$, but intermittency corrections will turn out to be larger by orders of magnitude. The value of D is again to be found in Table I.

In the case of the renormalized chain, the renormalized coupling constants $D(l)$, $1<l<N_\eta$, appear as additional parameters. They represent the effect of the parts of the tree which have been pruned [18]. However, they will not be adjustable parameters: At every cascade step they are fixed by the symmetry requirement that the mean value of the energy transfer into each of the eight subeddies be equal. It turns out that $D(l)$ is to very good accuracy determined by a fixed point: $D(l)=D^*$ for all levels l. The numerical value for D^*, which certainly depends on the other parameters, will also be given in Table I.

Comparison between the multifractal tree and the

TABLE II. The exponent deviations (or intermittency corrections) from classical scaling $\zeta_{\rm cl}(m)=m/3$ for the experiments of Anselmet *et al.* [7] and the model cascades of the second, third, and fifth lines of Table I. The scaling of the moments 2, 4, 6, 8, and 18 of $\Delta u(r)$ corresponds to moments 1, 2, 3, 4, and 9 of E_l, which is the quantity we actually computed. The last line quotes the results of simulations of the Navier-Stokes equation on the renormalized chain of Fig. 3. Here the moments of $\Delta u(r)$ are computed directly. The error bounds are statistical χ^2 errors.

Moment	2	4	6	8	18
Exponent deviation	$\delta\zeta(2)=\zeta(2)-\frac{2}{3}$	$\delta\zeta(4)=\zeta(4)-\frac{4}{3}$	$\delta\zeta(6)=\zeta(6)-2$	$\delta\zeta(8)=\zeta(8)-\frac{8}{3}$	$\delta\zeta(18)=\zeta(18)-6$
Experiment	0.04	0.00	−0.20	−0.45	−2.29
Linear chain $s=0,85$	0.0020±0.0001	−0.0035±0.0001	−0.0168±0.0002	−0.038±0.0004	−0.25±0.002
Linear chain $s=0,5$	0.0089±0.0007	−0.0061±0.002	−0.044±0.004	−0.103±0.006	−0.66±0.03
Multifractal tree, $s=0,15$	0.033±0.002	−0.0063±0.006	−0.28±0.01	−0.61±0.02	−3.21±0.3
Multifractal dynamics, Ref. [18]	0.032±0.0003	−0.0065±0.001	−0.30±0.01	−0.68±0.04	

pruned version is made in Figs. 5(a) and 5(b), where the first and fourth moments of E_l are shown. From the close agreement one can conclude that the renormalization procedure gives indeed a good representation of the complete tree. We can therefore move on to look at scaling in a somewhat longer pruned tree, from here on assuming that the scaling of the multifractal tree will not differ much from these results.

With this in mind, we simulate six levels of the renormalized chain, with the same parameters as before. We again average over 10^4 turnover times and omit the first and last levels in our power-law fit to the moments of E_l. Appreciable exponent deviations are now found. They are of the same order as the experimentally observed intermittency corrections. This confirms the idea that branching very significantly enhances intermittency.

V. DISCUSSION

One of the very convenient features of the present model is that it can be compared directly with the Navier-Stokes-generated dynamics on the same structures. As an example, we compare the energy distribution of the linear chain in the present model with the same quantity in the linear chain with Navier-Stokes-generated dynamics. In Fig. 6 the results for levels 1 and 2 are given, the present model (solid line) superimposed with the Navier-Stokes case (dotted line). The energy scale was adjusted to give the same mean value at level 1. It will be noted how well our simple model describes the higher-dimensional chaotic dynamics of the Navier-Stokes chain, at least when the latter is projected on the energy variable. Observe that the width of the distribution increases much faster towards higher levels than it should be expected from the tiny increases of the moments of E_l. The reason is that the variance $\sigma_{ll} = \langle E_l^2 \rangle - \langle E_l \rangle^2$ is the difference of two large numbers which almost cancel each other. So the slightly different scaling of $\langle E_l \rangle^2$ and $\langle E_l^2 \rangle$ is magnified greatly. Eventual-

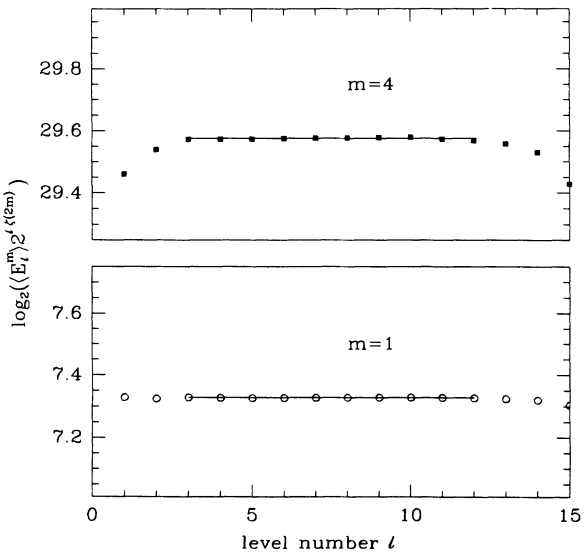

FIG. 4. Scaling of first (○) and fourth (■) moments of E_l for the linear chain, $s=0,85$ (see Table I). For velocity differences $\Delta u(r)$ this corresponds to moments 2 and 8. The power law $2^{-l\zeta(2m)}$ according to Table II has been subtracted, so only the scatter is visible. The straight line is a least-squares fit to levels 3–12 and is horizontal by construction.

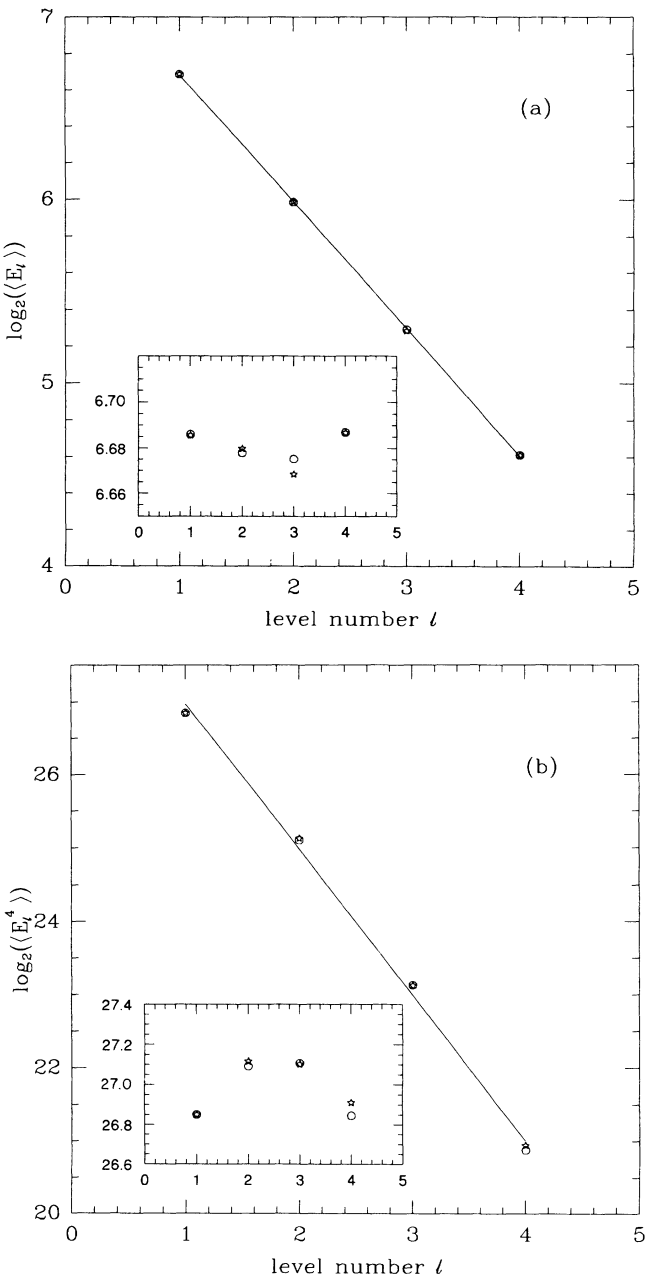

FIG. 5. (a) Comparison between the full multifractal tree (Fig. 1) and the renormalized chain (Fig. 3). Drawn is the average of the energy E_l for the tree (□) and for the chain (☆). In the inset $\langle E_l \rangle$ is multiplied with $2^{(l-1)\zeta(2m)}$ so that only the scatter is seen. The scale has been expanded to make some of the very small deviations visible. (b) Same as in (a), but for the fourth moment of the energy, corresponding to the exponent $\zeta(8)$. Due to the shortness of the cascade there are considerable end effects visible on the expanded scale of the inset. Yet the agreement between the tree and its renormalized version is very good.

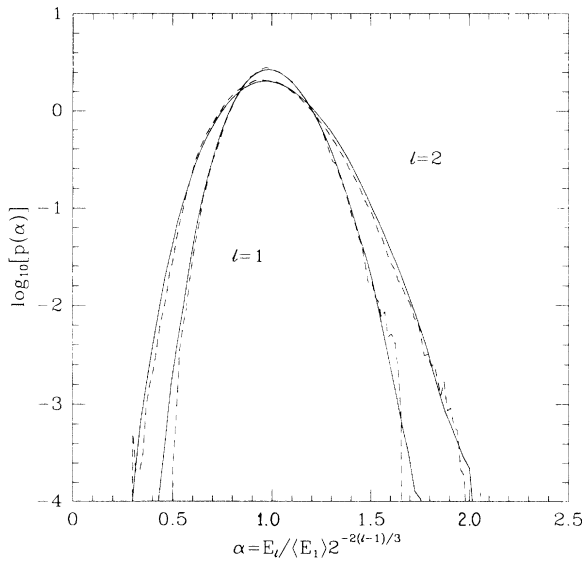

FIG. 6. The probability distribution of $E_l/\langle E_1\rangle 2^{-(2/3)(l-1)}$ for $l=1$ (largest scales) and 2 (next smaller scales). The full line is the result of the present simulations of the linear chain, cf. second row of Table I. The dashed line is the same distribution calculated in the Navier-Stokes-generated model of Ref. [20]. Due to much shorter averaging times, the convergence in the tails is not as good as in the stochastic model.

ly, for very large l, σ_{ll} will be determined solely by $\langle E_l^2\rangle$ and will grow much more slowly.

Another comparison, this time for the renormalized chain, is made in Table II. Again, by comparing the scaling exponents of the model (sixth) and the dynamics (seventh) one notes an impressive agreement.

This suggests that in the energy picture the statistics of small-scale flow is determined by only a few structural elements, as already discussed in the Introduction. Namely, (i) energy conservation (with correct local scaling of the transfers), (ii) return to absolute equilibrium, and (iii) fractal geometry. In our model, the implementation of (ii) was most *ad hoc*. The following simple dynamical justification can be given. Imagine a network of modes exchanging energy in the same fashion as in the present model, but with $p(V)=\frac{1}{2}$, independent of the ratios of the energies. In this case the fluctuations will be unbounded, as observed before. But if we introduce memory, for example, by saying that the direction of transfer be the same for two successive events, the process will tend to maximize the transfer. This is because transfer towards the maximum will be enhanced in the second step, while transfer away from it will be depleted. Therefore the system will tend to equipartition, where the transfers are maximized. This elaborates on the well-known fact that memory is essential for energy transfer [24].

We now turn to the perturbation theory of Sec. III in some more detail. So far all perturbative treatment of the turbulence problem [2–4] has given no indication of intermittency. The point demonstrated in those theories essentially is that the limit $L\to\infty$, $\eta\to 0$ can be performed at every finite order of the perturbation expansion. From this it follows directly on dimensional grounds that the classical scaling exponents are recovered. In the presence of an intermittent exponent correction the structure functions $D^{(m)}(r)$ take the form

$$D^{(m)}(r)=b_m(\varepsilon r)^{m/3}\left[\frac{r}{L}\right]^{\delta\zeta(m)}.$$

An exponent correction $\delta\zeta(m)=0$ therefore implies a "divergence" for $L\to\infty$. In our linearized approximation, this shows up as a logarithmic divergence, since via $l=\log_2(L/r)$ a linear dependence on the level number implies a logarithmic dependence on r/L. It is not clear why these terms do not seem to appear in the usual moment closures of the Navier-Stokes equation. One simplifying feature of the present model is its formulation in energy variables. In the velocity of our model [20], fluctuations in the individual amplitudes are very large, and all fixed points are highly unstable. Yet, the total energy of a shell is a "slow" variable of the system, being well described by fluctuations around a mean value as shown in Fig. 6. This corresponds to the emergence of the smallness parameter $\varphi_0^{1/2}$ for the noise strength. Hence even in the linear approximation one can make meaningful statements about the size of fluctuations.

We now make some quantitative comparisons between the prediction of the linear approximation and our numerical simulations of the linear chain. In Fig. 7, the comparison is made for the normalized variance $\hat{\sigma}_{ll}$ for a

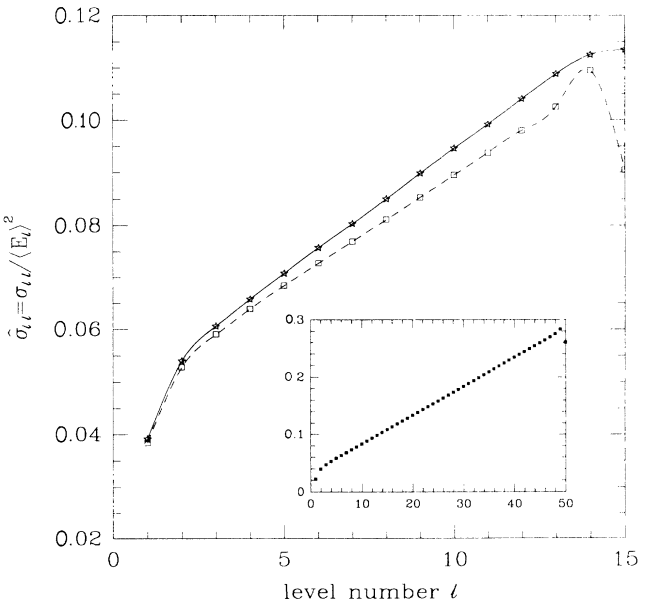

FIG. 7. Normalized variance $\hat{\sigma}_{ll}=\sigma_{ll}/\langle E_l\rangle^2$ of the energy vs level number l for the chain of 15 elements. The stars (☆) correspond to the simulations of the linear chain with $s=0.85$, the squares (□) to the low-noise expansion of Sec. III up to first order. The full and the dashed line, respectively, are drawn to guide the eye. The inset shows again the result of the low-noise expansion, but for 50 levels. The variance continues to grow linearly with level number.

chain of 15 elements. The slope of $\hat{\sigma}_{ll}$ determined from (3.23) for $N_\eta = 50$ and $s = 0.85$ is 5.066×10^{-3} (see inset), hence by (3.27) $\zeta(4) - 2\zeta(2) = 7.31 \times 10^{-3} +$ (higher orders). The simulation gives $7.5 \times 10^{-3} \pm 3 \times 10^{-4}$ for the same s. For $s = 0.5$ we have to compare $\zeta(4) - 2\zeta(2) = 0.020$ (perturbation theory) and $\zeta(4) - 2\zeta(2) = 0.024 \pm 0.003$ (simulation). We expect that higher and higher orders in δ will be necessary for an accurate calculation of higher-order moments. The convergence of the power series in δ still needs to be investigated.

Finally, to get more realistic values for the exponents, one needs to consider the multifractal tree instead of the chain. By pruning the tree as described in the Introduction, one ends up with a chain with *renormalized* chain elements. The corresponding matrices of the linearized problem are now banded matrices with eight upper and lower diagonal elements, instead of being tridiagonal. By comparing with our simulations we expect them to lead to exponent corrections which are larger by an order of magnitude.

In conclusion, we have constructed a dynamical model of turbulence which focuses on the geometrical aspects of the flow field. Details of the hydrodynamic interactions are only summarily described by a Langevin process and topological features are disregarded. While this puts severe restrictions on the range of phenomena which can be described within the model, it is shown to be sufficient to describe one of the most fundamental facts: the growth of intermittent fluctuations.

ACKNOWLEDGMENTS

The author is grateful to L. P. Kadanoff for suggestions on the manuscript and continued encouragement, and to X.-J. Wang for many valuable discussions on cascade models. During the last stages of preparing this manuscript he became aware of related work in progress by R. Benzi, G. Parisi, and L. Biferale. He thanks them for making some of their results available to him prior to publication. The author thanks the Department of Mathematics of the University of Chicago for their hospitality, and the Deutsche Forschungsgemeinschaft for support. He is also supported by the ONR under Grant No. N00014-90J-1194 and the NSF/DMR/MRL under Grant No. 8819860.

[1] A. N. Kolomogorov, C. R. Dokl. Acad. Sci. URSS **30**, 299 (1941); A. M. Obukhov, *ibid.* **32**, 19 (1941); C. F. von Weizsäcker, Z. Phys. **124**, 614 (1948); W. Heisenberg, *ibid.* **124**, 628 (1948); L. Onsager, Phys. Rev. **68**, 286 (1945).
[2] R. H. Kraichnan J. Fluid Mech. **5**, 497 (1959); Phys. Fluids **8**, 575 (1965).
[3] H. Effinger and S. Grossmann, Z. Phys. B **66**, 289 (1987).
[4] V. I. Belinicher and V. S. L'vov, Zh. Eksp. Teor. Fiz. **93**, 533 (1987) [Sov. Phys. JETP **66**, 303 (1987)].
[5] L. D. Landau and E. M. Lifshitz, *Fluid Mechanics* (Pergamon, Oxford, 1984).
[6] A. N. Kolmogorov, J. Fluid Mech. **13**, 82 (1962); A. N. Obukhov, *ibid.* **13**, 77 (1962).
[7] F. Anselmet, Y. Gagne, E. J. Hopfinger, and R. A. Antonia, J. Fluid Mech. **140**, 63 (1984).
[8] B. Castaing, Y. Gagne, and E. J. Hopfinger, Physica D **46**, 177 (1990).
[9] C. Meneveau and K. R. Sreenivasan, J. Fluid Mech. **224**, 429 (1991).
[10] C. DeDominicis and P. C. Martin, Phys. Rev. A **19**, 419 (1979).
[11] V. Yakhot and S. A. Orszag, J. Sci. Comput. **1**, 3 (1986).
[12] B. B. Mandelbrot, J. Fluid Mech. **62**, 331 (1974).
[13] U. Frisch, P. L. Sulem, and M. Nelkin, J. Fluid Mech. **87**, 719 (1978).
[14] R. Benzi, G. Paladin, G. Parisi, and A. Vulpiani, J. Phys. A **17**, 3521 (1984).
[15] C. Meneveau and K. R. Sreenivasan, Phys. Rev. Lett. **59**, 1424 (1987).
[16] J. Eggers and S. Grossmann, Phys. Rev. A **45**, 2360 (1992).
[17] J. Eggers and S. Grossmann, Phys. Lett. **153**, 12 (1991).
[18] J. Eggers and S. Grossmann, Phys. Lett. **156**, 444 (1991).
[19] R. H. Kraichnan, J. Fluid Mech. **59**, 745 (1973).
[20] J. Eggers and S. Grossmann, Phys. Fluids A **3**, 1958 (1991).
[21] R. M. Kerr and E. D. Siggia, J. Stat. Phys. **19**, 543 (1978).
[22] H. Risken, *The Fokker-Planck Equation* (Springer, Berlin, 1984).
[23] C. W. Gardiner, *Handbook of Stochastic Methods* (Springer, Berlin, 1985).
[24] R. H. Kraichman, J. Fluid Mech. **47**, 513 (1971).